GAMETE BIOLOGY

CrossMark

Simulated physiological oocyte maturation has side effects on bovine oocytes and embryos

Eduardo M. Razza[1] · Hanne S. Pedersen[2] · Lotte Stroebech[3] · Patricia K. Fontes[1] · Haja N. Kadarmideen[4] · Henrik Callesen[2] · Maria Pihl[5] · Marcelo F. G. Nogueira[1,6] · Poul Hyttel[5]

Abstract

Purpose Oocyte maturation is a complex process involving nuclear and cytoplasmic modulations, during which oocytes acquire their ability to become fertilized and support embryonic development. The oocyte is apparently "primed" for maturation during its development in the dominant follicle. As bovine oocytes immediately resume meiosis when cultured, it was hypothesized that delaying resumption of meiosis with cyclic nucleotide modulators before in vitro maturation (IVM) would allow the oocytes to acquire improved developmental competence.

Methods We tested the Simulated Physiological Oocyte Maturation (SPOM) system that uses forskolin and 3-isobutyl-1-methylxanthine for 2 h prior to IVM against two different systems of conventional IVM (Con-IVM). We evaluated the ultrastructure of matured oocytes and blastocysts and also assessed the expression of 96 genes related to embryo quality in the blastocysts.

Results In summary, the SPOM system resulted in lower blastocyst rates than both Con-IVM systems (30 ± 9.1 vs. 35 ± 8.7; 29 ± 2.6 vs. 38 ± 2.8). Mature SPOM oocytes had significantly increased volume and number of vesicles, reduced volume and surface density of large smooth endoplasmic reticulum clusters, and lower number of mitochondria than Con-IVM oocytes. SPOM blastocysts showed only subtle differences with parallel undulations of adjacent trophectoderm plasma membranes and peripherally localized ribosomes in cells of the inner cell mass compared with Con-IVM blastocysts. SPOM blastocysts, however, displayed significant downregulation of genes related to embryonic developmental potential when compared to Con-IVM blastocysts.

Conclusions Our results show that the use of the current version of the SPOM system may have adverse effects on oocytes and blastocysts calling for optimized protocols for improving oocyte competence.

Keywords In vitro maturation · SPOM · Bovine blastocyst · Gene expression · Ultrastructure

Introduction

In bovine oocytes, meiosis is initiated around Day 82 of gestation in the fetus. Subsequently this process is arrested in the diplotene, i.e., the germinal vesicle stage, until puberty when selected recruitment to resume meiosis occurs in the ovulatory follicle in response to gonadotrophins [1, 2]. The oocyte's basic competence for resuming meiosis and sustaining

✉ Eduardo M. Razza
eduardorazza@gmail.com

1 Department of Pharmacology, Institute of Bioscience, São Paulo State University (UNESP), Distrito de Rubião Junior s/n, Botucatu, São Paulo 18618970, Brazil

2 Department of Animal Science, Aarhus University, DK-8830 Tjele, Denmark

3 EmbryoTrans Biotech, Frederiksberg C, DK-1851 Copenhagen, Denmark

4 Department of Bio and Health Informatics, Technical University of Denmark, Kemitorvet, 2800 Kgs. Lyngby, Denmark

5 Department of Veterinary and Animal Sciences, University of Copenhagen, Frederiksberg C, Denmark

6 Department of Biological Sciences, School of Sciences and Languages, São Paulo State University (UNESP), Avenida Dom Antonio, 2100, Assis, São Paulo 19806900, Brazil

🖄 Springer

embryonic development is gradually built during the oocyte growth phase, when the oocyte grows from a diameter of approximately 30 to around 120 μm. Hence, it is estimated that bovine oocytes have acquired the competence for resuming meiosis at a diameter of approximately 100 μm and that they have acquired the further competence for completion of meiosis and for sustaining embryonic development to the blastocyst stage at around 110 μm corresponding to a follicle size of approximately 3 mm [3, 4]. It is, however, also clear that the oocytes undergo certain morphological changes during the development of the dominant follicle towards the time when the luteinizing hormone (LH) peak stimulates final oocyte maturation [5]. These changes in the oocyte of the dominant follicle have been referred to as oocyte "capacitation" or "pre-maturation" and it is believed that they contribute to enhanced oocyte competence and "prime" the oocyte for final maturation and further development. Accordingly, in vivo matured oocytes have higher developmental competence than their in vitro matured counterparts [6].

Before the LH surge, the natriuretic peptide precursor type C (NPPC) produced by mural granulosa cells stimulates the generation of cyclic guanosine monophosphate (cGMP) in the cumulus cells through stimulation of natriuretic peptide receptor 2 (NPR2) [7]. cGMP produced by the NPPC/NPR2 system is transferred to the oocyte via gap junctions and inhibits the activity of phosphodiesterase 3A (PDE3A) in the oocyte [8, 9], maintaining increased levels of cyclic adenosine monophosphate (cAMP) in the gamete and hereby sustaining meiotic arrest [7]. After the LH surge, the gap junctional contact is broken and cGMP levels decline allowing for the PDE3A to hydrolyze cAMP molecules in the oocyte, triggering meiotic resumption [10]. For the purpose of in vitro production of bovine embryos, the final stage of oocyte development is mimicked in vitro by removal of the cumulus-oocyte complex (COC) from antral follicles. Without the mural granulosa cell compartment, meiosis is resumed spontaneously and immediately. Hence, oocyte meiotic arrest is dependent on optimum concentrations of cAMP within the oocyte [11, 12].

In order to compensate for that, certain approaches aiming at improving oocyte developmental competence are based on two-step culture systems, which during the initial step block resumption of meiosis in order to allow for a mimic of oocyte capacitation and "prime" the oocyte for development [13–18]. Among the systems that have been developed, the most promising are those that pharmacologically inhibit or retard meiotic resumption with cyclic nucleotide modulators elevating the cAMP levels in the oocyte while sustaining functionality of the gap junction communication functionality (reviewed in [19].

However, little information is available about the morphological and molecular effects of such treatments on oocytes and resulting embryos. Therefore, our aim was to evaluate the potential effects of a treatment with cyclic nucleotide modulators prior to IVM (SPOM system) on the ultrastructure of oocytes and blastocysts as well as on the expression in the blastocysts of 96 genes related to embryo quality. Hence, we have challenged the SPOM system [19] against two different systems of conventional IVM (Con-IVM).

Material and methods

All chemicals and reagents were obtained from MilliporeSigma (Merck KGaA, Darmstadt, Germany) unless otherwise stated. In vitro production of embryos was performed in two different laboratories in Denmark: Aarhus University (AU-system) and University of Copenhagen (UCPH-system, EmbryoTrans Biotech). The in vitro performance of the SPOM-system was challenged against two different Con-IVM-systems. For the AU-system, we used a protocol that includes cattle serum (CS, Danish Veterinary Institute, DTU, Frederiksberg, Denmark) in its composition during IVM (15%) and embryo culture (5%). For the UCPH-system we used the whole package of commercially available serum-free ready-to-use media from IVF Bioscience (BO-Wash, BO-IVM, BO-IVF and BO-IVC). For the SPOM-system, we used the commercially available ready-to-use media (VitroWash, VitroMat, VitroFert and VitroCleave and VitroBlast) from IVF Vet solutions (Adelaide, Australia) for the whole procedure and performed the pre-maturation step according to manufacturer's instructions. Methods described are similar for all systems, unless otherwise stated.

In vitro embryo production

Oocyte collection for conventional and experimental IVM (Con-IVM and SPOM)

Bovine (*Bos taurus*) ovaries were collected from local slaughterhouses and then transported to the laboratory in 0.9% physiological saline solution in a thermo container at approximately 30–33 °C. COCs were aspirated from follicles 2 to 6 mm in diameter with a 19-G needle. The COCs were collected and washed once in Hepes-buffered Ml99 supplemented with 5 IU/mL heparin (LEO Chemical Factory, Ballerup, Denmark), 2.5 mg/mL amphotericin, and 1% CS (Danish Veterinary Institute, DTU, Frederiksberg, Denmark). COCs with minimum of 3–4 cumulus cell layers were selected for IVM and transferred in groups of 25 per well of 4-well dishes (Thermo Fisher Scientific, Roskilde, Denmark) containing 400 μl IVM medium (bicarbonate-buffered Ml99) supplemented with 10 IU/mL eCG and 5 IU/mL hCG (constituents of Suigonan Q, lntervet Scandinavia, Skovlunde, Denmark), 0.4 mM L-glutamine, 50 pg/mL gentamycin, and 15% CS and overlaid with 400 μl oil. Immature COCs were incubated for 24 h at 38.5 °C in 5% CO_2 in humidified air.

The SPOM-system

Briefly, COCs were selected to form groups of 50 and were pre-cultured for 2 h in 4-well plates containing 500 μL of VitroMat medium (IVF Vet Solutions, Adelaide, Australia) supplemented with the adenylate cyclase activator, forskolin (FSK, 100 μM), and the phosphodiesterase (PDE) inhibitor 3-isobutyl-1-methylxanthine (IBMX, 500 μM), according to [18]. After 2 h of pre-maturation, COCs were deeply washed (VitroWash media, IVF Vet Solutions, Adelaide, Australia) to completely remove SPOM medium and transferred to a well containing 500 μL of fresh VitroMat medium enriched with 100 mTU/mL recombinant human (rh) -FSH for IVM and cultured for 24 h.

In vitro fertilization and culture

Frozen-thawed semen from a Danish Holstein-Friesian bull (DAVID) was used for IVF in both facilities for all groups. Semen was thawed in 36 °C water and transferred into a centrifuge tube (Thermo Fisher Scientific, Roskilde, Denmark). The semen was washed in 2 mL Sperm-TALP (5.8 g/L NaCl, 0.2 g/L KCl, 0.04 g/L NaH_2OP_4, 0.3 g/L $CaCl_2$, 0.2 $MgCl_2$, 3.7 ml/L lactic acid, 1.4 g/L Hepes, 1.1 g/L Hepes-acid, 2.1 g/L $NaHCO_3$, 110 mg/L pyruvic acid, 100 mg/L gentamycin) by centrifugation for 10 min at 1500 rd/min. The supernatant was removed and the pellet re-suspended in 2 ml sperm-TALP. This procedure was repeated twice.

While washing the sperm, the oocytes were transferred to the IVF wells, 50 oocytes per well, containing 400 μL IVF medium (Sperm-TALP supplemented with 5 IU/mL heparin, 10 pM penicilliamine, 15 pM hypotaurine, and 1 pM epinephrine overlaid with 400 μl oil. Semen was added to the IVF wells in a concentration of 2,000,000 sperm/mL. The gametes were co-cultured for 20–22 h at 38.5 °C in 5% CO in humidified air.

Presumptive zygotes were vortexed to remove attached cumulus cells before transferred in groups of 25 per well of a 4-well dish containing 400 μL IVC medium. The embryos were cultured in a humidified mixture of 5% O_2, 5% CO_2, and 90% N_2 in air. The in vitro performance was assessed for rates of cleavage and blastocyst.

Transmission electron microscopy

Oocytes after IVM (minimum of 35 oocytes per group) and good-morphology expanded blastocysts (minimum of 10 equally-graded blastocysts per group) were collected from culture and fixed in 0.1 M Na-phosphate buffer (pH 7.3) containing 3% glutaraldehyde for 1 h at room temperature and stored at 4 °C in Na-phosphate buffer for later preparation for transmission electron microscopy (TEM) (Figs. 1 and 2).

Glutaraldehyde-fixed specimens were embedded in 4% agar at 45 °C (Bacto Agar; Difco Laboratories, Detroit, MI), post-fixed in 1% OsO4 in 0.1 M Na-phosphate buffer for 1 h at room temperature and washed briefly in 0.1 M Na-phosphate buffer. Embedded oocytes and embryos were stained with 1% uranyl acetate (Polysciences, Niles, IL) and dehydrated serially in ethanol. Subsequently, they were washed in propylene oxide twice for 10 min, further embedded in Epon (TAAB 812 embedding resin; VWR, West Chester, PA) and polymerized for 48 h at 60 °C for semithin sectioning. Semithin (2 μm) sections were cut serially through the oocytes/embryos on an ultramicrotome (Reichert Ultracut S; Leica, Microsystems, Wetzlar, Germany) using glass knives produced from a glass knife maker (LKB Bromma 7800; Leica Microsystems). Semithin sections were stained with 1% toluidine blue and examined under bright-field microscopy.

Sections of interest were re-embedded for ultrathin sectioning (60–80 nm) and sectioned using a diamond knife (Jumdi; Canemco and Marivac, Quebec, Canada) as previously described [20]. Ultrathin sections were contrast-stained using 2% uranyl acetate and lead citrate (Merck, Rahway, NJ), collected on 150 mesh copper grids covered with parlodion/amylacatate film (EMS; Fort Washington, PA) and examined on a transmission electron microscope (CM100, Philips, Darmstadt, The Netherlands) for assessment of ultrastructure of oocytes and blastocysts.

Analyses of cytoplasmic organelle parameters

Only matured oocytes, represented by a metaphase II plate and presence of polar body in the semithin sections, were further processed for TEM (minimum of 25 oocytes per group). Electron micrographs of areas representing randomly chosen areas of peripheral ooplasm (zone within 10 μm of the oocyte plasma membrane) and central ooplasm were analyzed. Quantitative analyses were performed in oocytes by standard stereological methods [21], which consisted in the placement of a test-grid over an electron micrograph adapted in the *Fiji* plugin software, an open source package from the image processing software *Image-J* (Wayne Rasband, National Institutes of Health, Bethesda, MD, USA, available for free download at https://imagej.nih.gov/nih-image/index.html) according to [22]. The distance between each adjacent cross-points on the grid provided an area of 0.25 μm^2. The surface area density (surface area of organelle per unit volume of cytoplasm; $\mu m^2/\mu m^3$), volume density (volume of organelle per unit volume of cytoplasm; $\mu m^3/\mu m^3$) and/or numerical density (number of organelle per unit volume of cytoplasm; number/μm^3) were calculated for selected organelles [23, 24]. For simplicity, the numerical density of organelles is presented as number/1000 μm^3 of oocyte volume. The relationship between the peripheral and central regions was

Fig. 1 Transmission electron micrographs of mature bovine oocytes produced by the Con-IVM system (**A**, **B**, and **C**) or by the SPOM system (**D**, **E**, and **F**). **A** Mature oocyte identified by the presence of a polar body (PB). Note the low density and central localization of vesicles. Inset: light micrograph of a mature oocyte. **B** Oocyte showing cortical granules located at solitary positions in the periphery of the ooplasm. **C** Detail from oocyte showing the close interaction of mitochondria (M) and a vesicle (V) with the smooth endoplasmic reticulum (SER). **D** Mature oocyte, identified by the PB, showing high density and more even distribution of vesicles. Inset: light micrograph of mature oocyte. **E** Oocyte with a big cluster of cortical granules. **F** Detail from oocyte showing mitochondria (M) with less prominent association with smooth endoplasmic reticulum (SER)
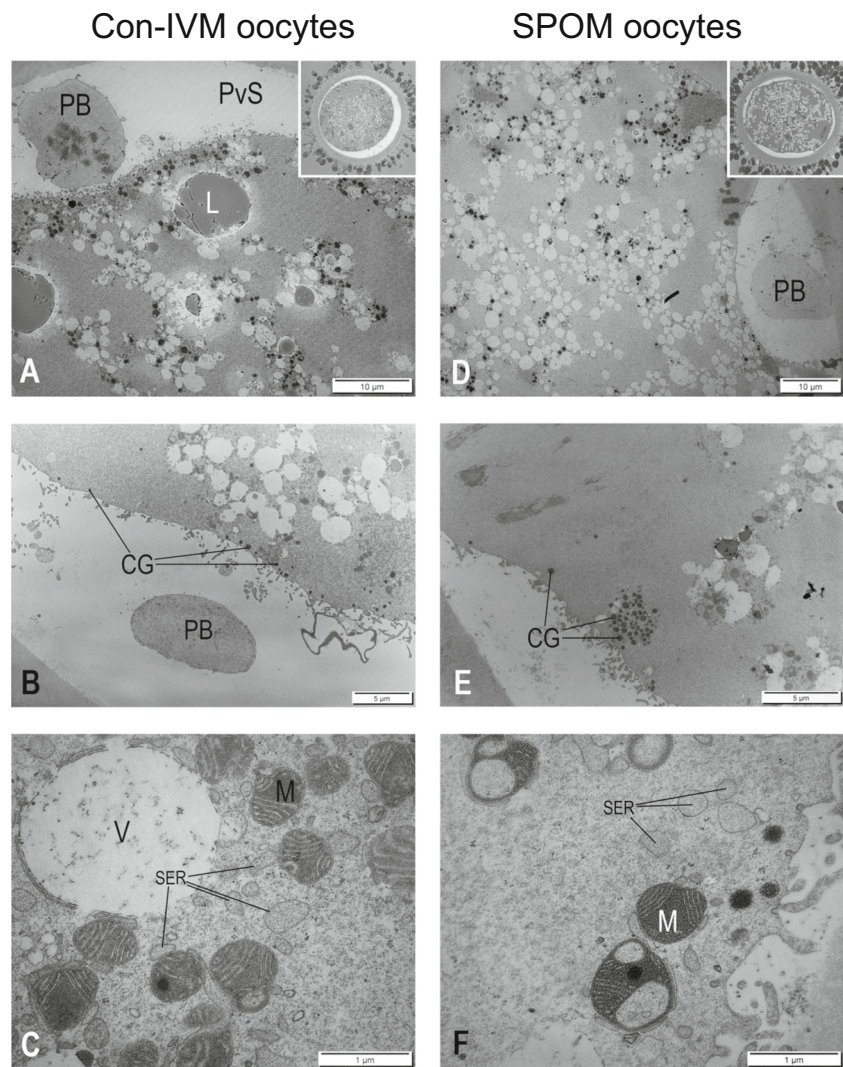
calculated for each oocyte and the resulting index was statistically compared between groups. Only blastocysts being evaluated as having good quality by stereomicroscopy were processed for TEM (minimum of ten equally-graded blastocysts per group). Representative areas of the trophectoderm (TE) and the inner cell mass (ICM) were analyzed.

Gene expression

Collection of blastocyst samples

Blastocysts were collected individually from cultures at 180 h post-insemination and stored in small volume of PBS-PVP at − 80 °C until RNA extraction. We selected only grade 1 good-quality expanded blastocysts without morphological signs of degeneration [25]. Embryos were combined to form pools of three blastocysts, defined as biological replicate and submitted to RNA extraction.

RNA isolation and reverse transcription

Total RNA from each pool of blastocysts was extracted with the PicoPure RNA Isolation kit (Life Technologies, Foster City, CA, USA) following the manufacturer's protocol. DNAse treatment was performed in all samples during RNA isolation as instructed by the manufacturer. Extracted RNA was stored at − 80 °C until further analysis by reverse transcription quantitative real time polymerase chain reaction (RT-qPCR). RNA concentration was quantified by a spectrophotometer (Nanodrop, ThermoFischer Scientific, MA, USA), and a 2100 Bioanalyzer apparatus (Agilent Technologies, CA, USA) was used to assess RNA quality with RNA Pico Chips (Agilent Technologies). All analyzed blastocyst samples had a RNA integrity number (RIN) ≥ 7. We used 100 ng of each sample to reverse transcription and the cDNA synthesis was performed using High Capacity Reverse Transcription kit (Applied Biosystems, Foster City, CA, USA), following manufacturer's instructions.
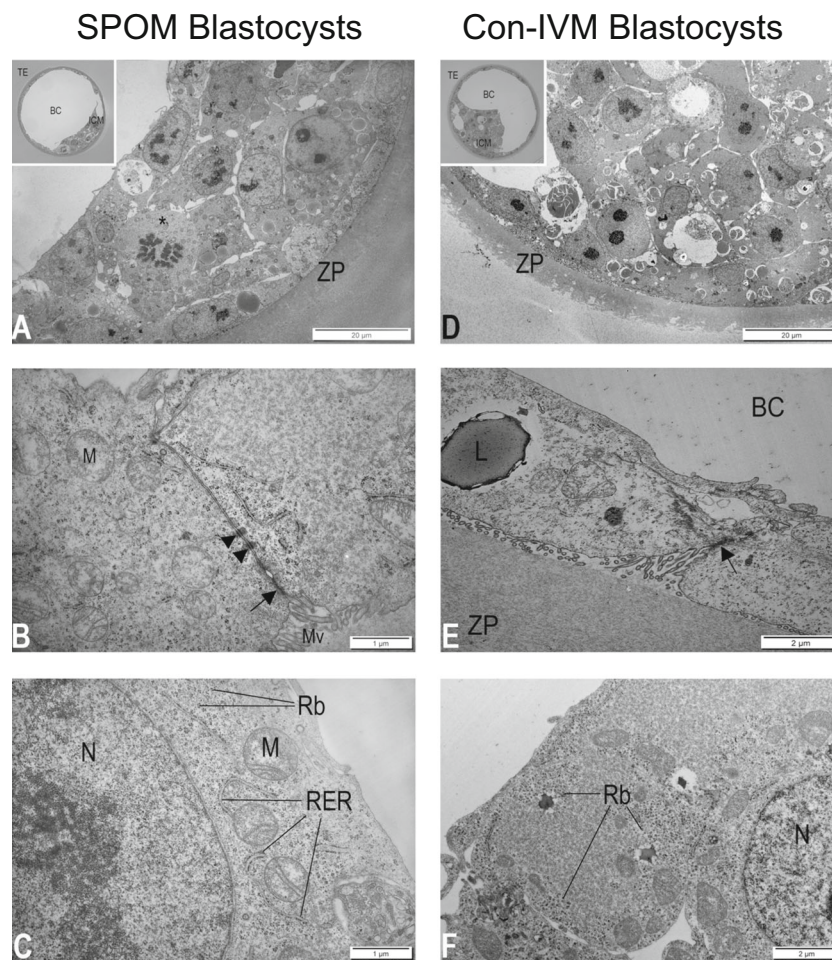
SPOM Blastocysts   Con-IVM Blastocysts

Fig. 2 Transmission electron micrographs of bovine blastocysts produced after oocyte maturation via conventional IVM (Con-IVM; **A**, **B** and **C**) and via the simulated-physiological oocyte maturation (SPOM; **D**, **E** and **F**) system. **A** Inner cell mass, polar trophectoderm, and zona pellucida (ZP) of blastocyst. Inset: light micrograph of blastocyst with inner cell mass (ICM), trophectoderm (TE), and blastocyst cavity (BC). **B** Detail showing the connection between two trophoblasts with a well-developed tight junction (arrow) followed by two desmosomes (arrowheads). **C** Detail of inner cell mass cell showing nucleus (N) and rough endoplasmic reticulum (RER) in close association with the mitochondria (M). Note that the ribosomes (Rb) are attached to RER and distributed freely throughout the cytoplasm. **D** Inner cell mass, polar trophectoderm, and zona pellucida (ZP) of blastocyst. Inset: light micrograph of blastocyst with inner cell mass (ICM), trophectoderm (TE), and blastocyst cavity (BC). **E** Detail showing the connection between two trophoblasts with undulating lateral plasma membranes and less developed tight junction (arrow). Note the lipid droplet (L) in the trophoblast. **F** Detail of inner cell mass cell showing nucleus (N) and ribosomes (Rb) mostly located in the periphery of the cells of the cytoplasm

Pre-amplification and real time polymerase chain reaction

Gene expression analysis of bovine blastocysts was performed using Applied Biosystems™ TaqMan® Assays, specific for *Bos taurus*. We analyzed the mRNA abundance of genes per functional categories for blastocysts (for gene symbols, names and further details, see supplementary material 1). Prior to RT-qPCR thermal cycling, each sample was submitted to sequence-specific pre-amplification process as follows: 1.25 μL assay mix (TaqMan® Assay was pooled to a final concentration of 0.2× for each of the 96 assays), 2.5 μL TaqMan PreAmp Master Mix (Applied Biosystems, #4391128), and 1.25 μL cDNA (5 ng/μL). The reactions were activated at 95 °C for 10 min followed by denaturing at 95 °C for 15 s, annealing and amplification at 60 °C for 4 min for 12 cycles. These pre-amplified products were diluted fivefold prior to RT-qPCR analysis.

Assays and pre-amplified samples were transferred to an integrated fluidic circuits (IFC) plate. For gene expression analysis, the sample solution prepared consisted of 2.25 μL cDNA (pre-amplified products), 2.5 μL of TaqMan Universal PCR Master Mix (2×, Applied Biosystems) and 0.25 μL of 20× GE Sample Loading Reagent (Fluidigm); and the assay solution: 2.5 μL of 20× TaqMan Gene Expression Assay (Applied Biosystems) and 2.5 μL of 2× Assay Loading Reagent (Fluidigm). The 96.96 Dynamic Array™ Integrated Fluidic Circuits (Fluidigm) chip was used for data collection. After priming, the chip was loaded with 5 μL of each assay

solution and 5 μL of each sample solution before being loaded into an automated controller that prepares the nanoliter reactions.

The RT-qPCR thermal cycling was performed in the Biomark HD System (Fluidigm, South San Francisco, CA, USA) using the protocol TaqMan GE 96 × 96 Standard, that consisted of one stage of Thermal Mix (50 °C for 2 min, 70 °C for 20 min and 25 °C for 10 min) followed by a Hot Start stage (50 °C for 2 min and 95 °C for 10 min), followed by 40 cycles of denaturation (95 °C for 15 s), primer annealing, and extension (60 °C for 60 s).

Statistical analysis

Data from in vitro production performance and ultrastructure assessment of oocytes and blastocyst were analyzed using Proc GENMOD of SAS software (2003). Individual ultrastructural images were analyzed qualitatively/ morphologically and quantitatively via stereological evaluation. Stereological quantitative data were analyzed with t test and are presented as mean ± standard error (SEM). The data for central and peripheral regions were pooled for the endpoints where significant differences were not observed. For RT-qPCR data, we calculated the ΔCt values relative to the geometric mean of the best housekeeping genes (GAPDH, PPIA and SF3A1) in the 96-gene set. Fold-changes were calculated as $2^{-\Delta Ct}$. Data were analyzed using JMP (Version: 13.0, SAS Institute Inc., Cary, NC, USA). We considered genes in SPOM group to be up or downregulated in relation to the control group. Statistical significance was determined based on a P value ≤ 0.05.

Results

Developmental competence

The in vitro performance (rates of cleavage and blastocyst, morphology grading, and kinetics) of embryo production from the two different labs (SPOM vs. UCPH-system: 4 replicates and SPOM vs. AU-system: 8 replicates) is presented in Table 1. Groups of Con-IVM reached higher blastocyst rates in both comparisons: SPOM vs. UCPH-system (29 ± 2.6 vs. 38 ± 2.8) and SPOM vs. AU-system (30 ± 9.1 vs. 35 ± 8.7).

Qualitative morphologic observations

The results of the ultrastructural evaluations were identical for UCPH-IVM and AU-IVM systems. Hence, a common presentation of the differences noted between the Con-IVM and SPOM systems is given. A few (three out of 35) SPOM-oocytes presented a germinal vesicle, but exclusively oocytes presenting a metaphase II and first polar body in the semithin sections were processed for further ultrastructural assessment

and quantitative investigations. Stereological results on individual comparison, i.e., SPOM vs. UCPH-IVM and SPOM vs. AU-IVM did not show statistical significance (data not shown), even though group comparison behaved very similarly. Hence we decided to pool samples in a broader systematic comparison, which are the SPOM samples (produced in both UCPH and AU labs) versus Con-IVM samples (compiled Con-IVM from both labs). By doing so we could illustrate the differences presented in Fig. 3 and Table 2.

Con-IVM oocytes presented a well-organized metaphase-II plate, a first polar body, a preferentially central accumulation of vesicles (Fig. 1A), peripheral solitary localization of cortical granules (Fig. 1B), and large smooth endoplasmic reticulum (SER) clusters. Moreover, they displayed a close spatial association between SER and the typically hooded mitochondria (Fig. 1C), lipid droplets, and vesicles. SPOM oocytes displayed morphological signs of incomplete cytoplasmic maturation including a more homogeneous distribution of mitochondria, vesicles, and lipid droplets (Fig. 1D) and presence of clusters of cortical granules (Fig. 1E). Also, the SER association with mitochondria was less prominent (Fig. 1F).

The Con-IVM and SPOM blastocysts displayed rather similar morphology with only minor differences (Fig. 2A, D). SPOM blastocysts often displayed parallel undulations of the lateral plasma membranes of adjacent TE cells with apparently less developed tight junctions and less desmosomes (Fig. 2B, E), the presence of lipid droplets in the TE cells, and unusual spatial localization of ribosomes and polyribosomes to the cortical cytoplasm of cells of the ICM (Fig. 2C, F).

Quantitative stereological data

Again, the results of the quantitative ultrastructural evaluation were identical for UCPH-IVM and AU-IVM-systems. Hence, a common presentation of the differences noted between the SPOM and the Con-IVM systems is given.

Data from the surface area density (surface area of organelle per unit volume of cytoplasm; $\mu m^2/\mu m^3$), volume density (volume of organelle per unit volume of cytoplasm; $\mu m^3/\mu m^3$), and numerical density (number of organelle per unit volume of cytoplasm; number/μm^3) of cortical granules, lipids, vesicles, large smooth endoplasmic reticulum (SER) clusters and mitochondria are presented for Con-IVM and SPOM oocytes in Table 2.

Con-IVM oocytes presented significantly more cortical granules and mitochondria and the volume and surface area of large SER clusters were also significantly higher. On the contrary, both the number and volume of vesicles were increased in SPOM oocytes.

Differences between Con-IVM and SPOM oocytes were also noted with respect to the localization of organelles and inclusions (Fig. 3). Hence, lipid droplets were evenly

Table 1 In vitro performance (rates (% ±SD) of cleavage and blastocyst) of bovine embryos produced by the simulated-physiological oocyte maturation (SPOM) system compared with two conventional in vitro maturation systems (Con-IVM: UCPH-system and AU-system)

Group	No. of COC	Cleavage % ±SD	Blastocyst % ±SD
University of Copenhagen			
Con-IVM (UCPH-system)	412	85 ± 1.7	38 ± 2.8[a]
SPOM	407	81 ± 2.3	29 ± 2.6[b]
Aarhus University			
Con-IVM (AU-system)	685	80 ± 17.9	35 ± 8.7[a]
SPOM	686	53 ± 13.7	30 ± 9.1[b]

COC = cumulus-oocyte complex

distributed in Con-IVM oocytes but attained a more peripheral localization in SPOM oocytes, vesicles were centrally localized in Con-IVM oocytes but attained a more even distribution in SPOM oocytes and large SER clusters were peripherally localized in Con-IVM oocytes but attained a more even distribution in SPOM oocytes. No differences were noted with respect to the localization of mitochondria.

Gene expression

Differentially expressed genes indicated downregulation of ten genes in SPOM blastocysts as compared with their Con-IVM UCPH-System counterparts: beta-2-microglobulin (*B2M*), regulator of G protein signaling 2 (*RGS2*), aldo-keto reductase family 1 member B1 (*AKR1B1*), glucose-6-phosphate dehydrogenase (*G6PD*), heat shock 60 kDa protein 1A (*HSPD1*), hypoxia inducible factor 1 alpha subunit (*HIF1A*), platelet-activating factor (*PAF1*), thioredoxin (*TXN*), superoxide dismutase 1 (*SOD1*), and interferon-induced transmembrane protein 3 (*IFITM3*). Two genes were, on the other hand, upregulated in SPOM blastocysts: solute carrier family 2, member 5 (*SLC2A5*), and actin beta (*ACTB*) (Fig. 4).

When analyzing SPOM blastocysts with their Con-IVM AU-System counterparts, three genes were downregulated: fatty acid elongase 5 (*ELOVL5*), stearoyl-CoA desaturase (*SCD*), and acyl-CoA synthetase long-chain family member 6 (*ACSL6*) (Fig. 5) and none was upregulated.

Discussion

Fully mature oocytes from an ovulatory follicle at about 24 h after the LH peak normally should present the cortical granules distributed at solitary positions along the oolemma, lipid droplets, and mitochondria attained in a more central location in the ooplasm leaving a rather organelle-free peripheral zone in which the most prominent features are large clusters of SER [4]. In our work, we compared two different IVM systems for IVP of bovine embryos. Our analyses revealed ultrastructural deviations of SER, mitochondria, lipid droplets, vesicles, and cortical granules in oocytes arising from the SPOM-system

and, moreover, ultrastructural deviations were also observed in the resulting blastocysts combined with deviant gene expression profiles.

In our experiments, the in vitro performance of the SPOM-system was inferior to that of the Con-IVM in two different comparisons (UCPH-system and AU-system). Previous studies using the SPOM-system, or similar systems with FSK and IBMX, have reported successful results of this approach in several species [18, 26–32]. Conversely, other studies have shown neutral or compromised results using SPOM-like approaches [33–35]. Hence, in the light of this inconsistency, we attempted to evaluate the effect and efficiency of the SPOM-system by ultrastructural and gene expression analyses; methodologies that have not been applied earlier.

An important ultrastructural feature of competent fully mature oocytes is the peripheral solitary distribution of the cortical granules in the ooplasm [36]. These organelles are extremely important for proper zygote formation after fertilization, since cortical granules contain ovastacin, a protease that cleaves zona pellucida protein-2 and induces the hardening of the zona preventing polyspermy [37, 38]. Our quantitative and qualitative ultrastructural observations clearly demonstrated that the number of solitary cortical granules in the cortical ooplasma was significant lower in SPOM oocytes when compared to Con-IVM. Furthermore, the granules remained clustered to a higher degree in the SPOM oocytes. These features may be reflected in the lower blastocyst rates obtained in the SPOM group.

Another feature that may negatively affect oocyte competence and fertilization is the reduced number of mitochondria observed in the SPOM oocytes [39]. It is known that high numbers of mitochondria increase adenosine triphosphate production during oocyte maturation and are associated with improved oocyte quality [40, 41]. Our findings of a reduced mitochondrial numerical density in the SPOM oocytes indicate a compromised energy metabolism possibly reducing embryonic outcome.

Since we have only selected the best quality blastocysts resulting from both the SPOM and the Con-IVM-systems, ultrastructural deviations were less likely to be found, as detrimental effects would have manifested themselves earlier

Fig. 3 Organelle localization (central versus periphery) in oocytes after in vitro maturation with the conventional maturation system (Con-IVM) or the simulated-physiological oocyte maturation (SPOM) system. SER: smooth endoplasmic reticulum. *P* value of comparison between groups for each structure is described in parenthesis. Considering significant differences as $P \leq 0.05$, only mitochondria localization did not differ between groups
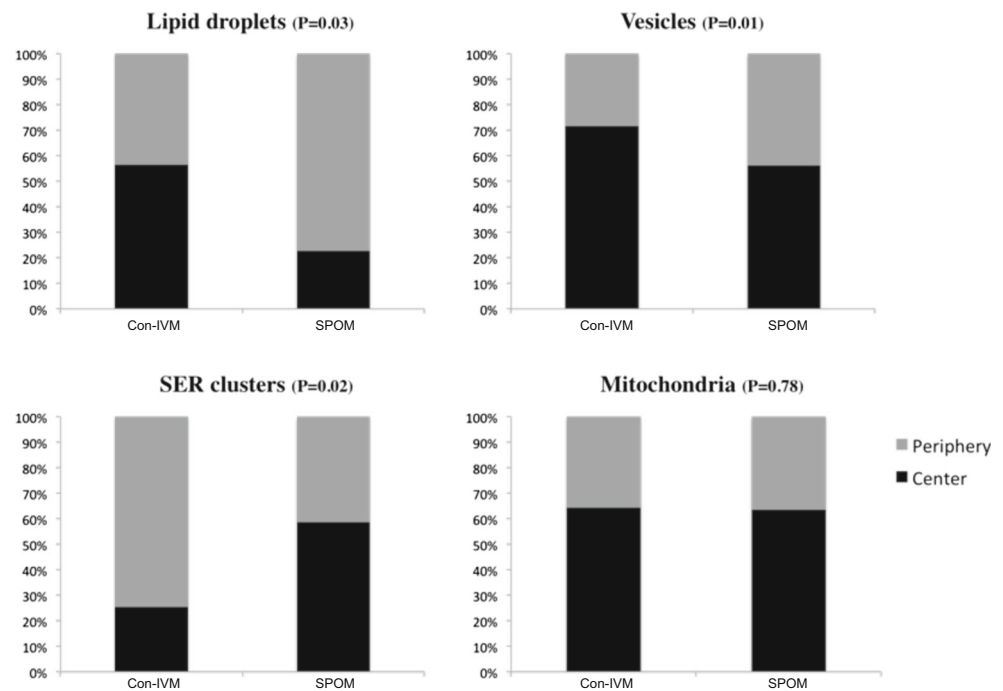
during development. Nevertheless, our findings indicate subtle ultrastructure modifications that might have persisted in the SPOM group all the way to the stereo microscopically excellent blastocyst stage. Hence, blastocysts produced from oocytes submitted to the SPOM-system, often presented undulations in the plasma membrane of neighboring TE cells with less developed tight junctions and desmosomes. Proper formation and function of such junctions have been reported to better maintain the structural integrity and regulate the internal environment of the embryos [42].

Ribosomes and polyribosomes are common in embryonic cells [43], but we found differences between groups regarding the spatial ribosomal organization in the inner cell mass (ICM) of blastocysts. Ribosomes were found spread throughout the cytoplasm in ICM cells in Con-IVM blastocysts, while SPOM blastocysts presented ribosomes organized preferably in the periphery of the ICM cells. Reasons accounting for these findings are speculative, but previous research has suggested that ribosomes are redistributed such that they accumulate at the site of protein synthesis [44–46] and also according to the

Table 2 Volume (percent of ooplasm), surface density (Mean ± SEM, $\mu m^2/\mu m^3$ of ooplasm) number (Mean ± SEM, per 1000 μm^3 of ooplasm) of lipids, vesicles, large clusters of smooth endoplasmic reticulum (SER), and mitochondria in matured oocytes from the simulated-physiological oocyte maturation (SPOM; $n = 15$) system compared with the conventional in vitro maturation systems (Con-IVM; $n = 17$)

Organelle	Parameter (*P* value)	Con-IVM (Mean ± SEM)	SPOM (Mean ± SEM)
Cortical granule	Number (/1000 μm^3) ($P = 0.04$)	2.21 ± 0.9[a]	1.27 ± 0.2[b]
Lipid	Volume density (%) ($P = 0.92$)	1.52 ± 6.9	1.48 ± 1.0
	Surface density ($\mu m^2/\mu m^3$) ($P = 0.98$)	0.15 ± 0.06	0.14 ± 0.10
	Number (/1000 μm^3) ($P = 0.64$)	13 ± 4.9	14 ± 8.4
Vesicle	Volume (%) ($P = 0.04$)	13.14 ± 6.5[a]	24.79 ± 12.9[b]
	Surface density ($\mu m^2/\mu m^3$) ($P = 0.88$)	1.31 ± 0.65	2.47 ± 1.29
	Number (/1000 μm^3) ($P = 0.007$)	140 ± 77.7[a]	244 ± 111.8[b]
Large SER cluster	Volume (%) ($P = 0.03$)	3.62 ± 2.2[a]	1.48 ± 1.6[b]
	Surface density ($\mu m^2/\mu m^3$) ($P = 0.04$)	0.36 ± 0.22[a]	0.14 ± 0.16[b]
	Number (/1000 μm^3) ($P = 0.06$)	5 ± 2.4	3 ± 2.0
Mitochondrion	Volume (%) ($P = 0.44$)	6.91 ± 3.5	5.85 ± 2.1
	Surface density ($\mu m^2/\mu m^3$) ($P = 0.52$)	0.69 ± 0.35	0.58 ± 0.21
	Number (/1000 μm^3) ($P = 0.03$)	170 ± 92.5[a]	119 ± 66.6[b]

Values with different superscripts are different ($P < 0.05$). Analyses were done on proportions, not percentages
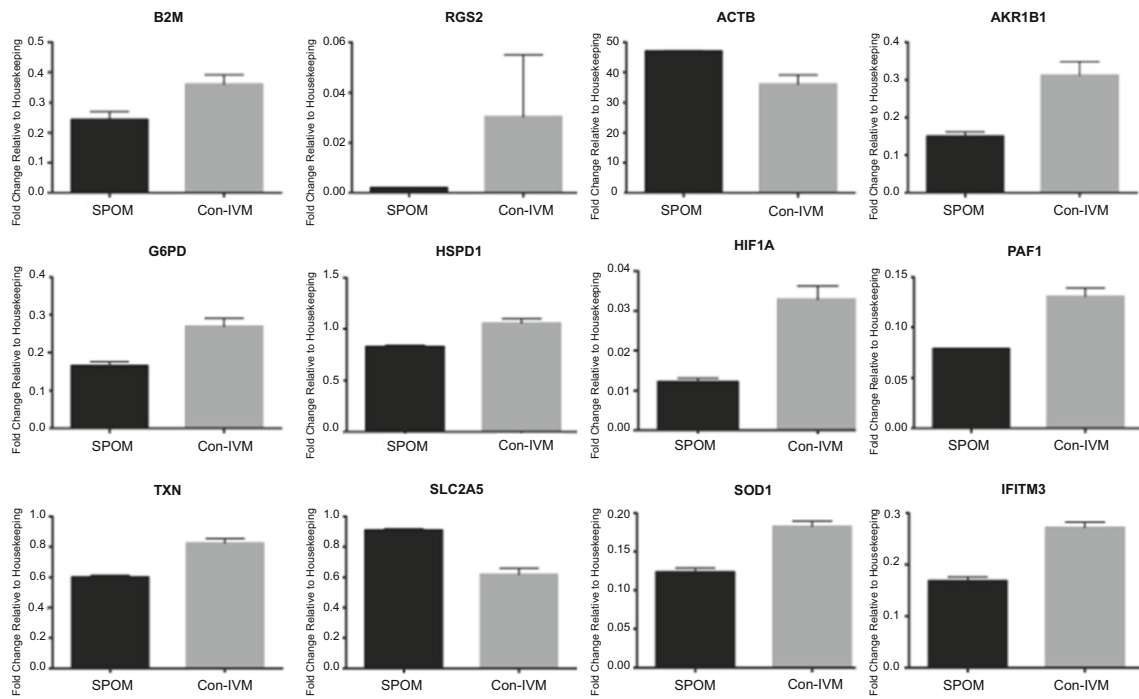
Fig. 4 Differential gene expression of blastocysts produced in vitro from COCs submitted to simulated-physiological oocyte maturation (SPOM) system or conventional in vitro maturation (Con-IVM) using the UCPH-System (performed at University of Copenhagen). Data represent the fold-change of level of expression relative to housekeeping genes. Results are least-squares means + SEM. The effect of treatment was $P \leq 0.05$ for all genes in the figure

stage of the cell cycle [47], implying that the ribosome population undergoes dynamic non-random movement as required. The consequences for such ribosome segregation within the inner cell mass of SPOM blastocysts may reflect further at the level of protein synthesis.

We assessed blastocysts for the expression of 96 genes related to embryo quality. Comparing SPOM with Con-IVM using the UCPH-system, we found 12 genes to be differentially expressed between groups. The same comparison of SPOM versus Con-IVM with the AU-system showed differential gene expression of only three genes. None of the genes expressed differentially in the comparison with SPOM were common between the UCPH and AU-system indicating that gene expression in blastocysts may vary greatly between

production systems including a complexity of all aspects involved in IVM, IVF, and IVC. Hence, differential gene expression data observed in our work indicates that variation in transcripts may be related to differential culture conditions during IVM, IVF, and IVC rather than to the SPOM systems itself.

Specifically, we found the genes *B2M, RGS2, AKR1B1, G6PD, HSPD1, HIF1A, PAF1, TXN, SOD1,* and *IFITM3* to be upregulated and *SLC2A5* and *ACTB* to be downregulated in the UCPH-system blastocysts as compared with SPOM. *G6PD* encodes the main rate-limiting enzyme regulating the use of glucose by the pentose-phosphate pathway (PPP), which is known to increase significantly from morulae to blastocyst stage [48]. The main intracellular reductant
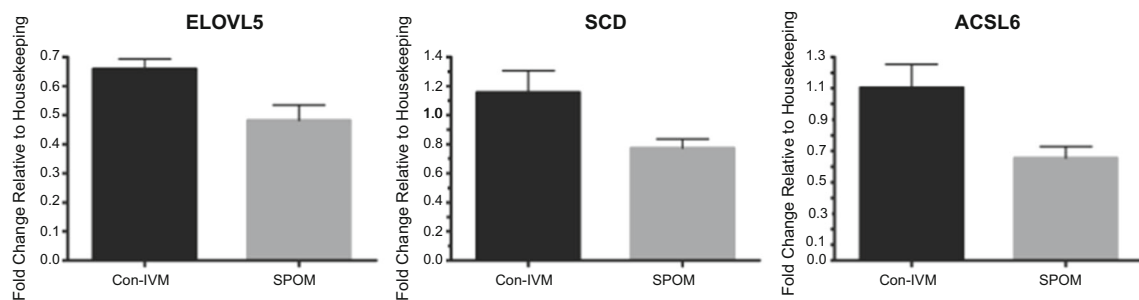

Fig. 5 Differential gene expression of blastocysts produced in vitro from COCs submitted to simulated-physiological oocyte maturation (SPOM) system or conventional in vitro maturation (Con-IVM) using the AU-System (performed at Aarhus University). Data represent the fold-change of level of expression relative to housekeeping genes. Results are least-squares means + SEM. The effect of treatment was $P \leq 0.05$ for all genes in the figure

generated by the PPP reaction is NADPH, which, together with super oxide (SOD) enzymes, has an important action in embryo protection from free oxygen radicals [49]. As the mRNA abundance of both *G6PD* and *SOD1* were increased in Con-IVM blastocysts (UCPH-system), it may imply a better use of the metabolic machinery for these blastocysts. On the other hand, the expression of *SLC2A5*, encoding for enzymes of the glycolysis pathway, shown to be important for embryo development [50], was increased for the SPOM blastocysts, potentially indicating the use of a different metabolic pathway for the embryonic energy consumption.

In an elegant work, Ghanem et al. [51] investigated the transcript signatures of biopsies from in vivo- and in vitro-derived embryos with developmental competence to term. In that work, the downregulation of *B2M, RGS2,* and *TXN,* as observed for SPOM blastocysts in our experiment, was related to pregnancy loss. On the other hand, the upregulation of *AKR1B1* and *HSPD1* and the downregulation of *ACTB,* as observed in Con-IVM blastocysts (UCPH-system) were found in embryos resulting in no pregnancy [51].

Embryos lacking PAF1 complex expression are developmentally disabled [52], therefore crucial for embryonic competence. In our experiments, SPOM blastocysts presented downregulation of *PAF1.* Another important marker is *IFITM3,* which is present in the ICM of bovine blastocysts [53]. *IFITM3* was also downregulated in SPOM blastocysts, suggesting compromised embryonic competence as compared to Con-IVM embryos (UCPH-System).

The gene expression of hypoxia-inducible factors (HIFs) is known to be affected by different oxygen concentrations [54]; however, this experiment was conducted under low oxygen tension as a whole. *HIF1A* also contributes to the expression of the main enzyme of anaerobic conversion of pyruvate into lactate, lactate dehydrogenase A [55, 56], that promotes anaerobic glycolysis in tumor cells [57, 58] and was previously found to be downregulated in bovine ICM cells [59]. In our experiments, *HIF1A* was downregulated in SPOM blastocysts, suggesting that different metabolic pathways might be operating in SPOM when compared to Con-IVM blastocysts.

We have shown recently that treating COCs with cAMP modulators prior to IVM alters the lipid composition of mature oocytes and embryos [60]. In the present work, when challenging the SPOM-system with the Con-IVM AU-system, we found that three transcripts related to lipid metabolism within the cell, *ELOVL5, SCD,* and *ACSL6,* were downregulated in blastocysts from SPOM group. Triglycerides (TAG) are stored as lipid droplets in the cytoplasm of mammalian cells and work as a source of energy for the early embryonic development [61, 62]. Family members of SCD, ACSLs and ELOVLs, seem to be involved in the lipid metabolism in bovine embryos. The ACSL family induces long-chain fatty acids to generate long-chain acyl-CoA resulting in the synthesis of various lipid species including TAG [63]. The ELOVL

family acts on the generation of very long chains of fatty acids [64] and SCD catalyzes important pathways of monounsaturated fatty acids [65]. It is possible that the differential regulation in genes related to the lipid metabolism have contributed to the presence of lipid droplets observed in the TE cells of blastocysts produced from SPOM oocytes.

Conclusion

In summary, oocytes submitted to simulated-physiological oocyte maturation system present qualitative and quantitative ultrastructural deviations with respect to abundance (SER, mitochondria, vesicles, and cortical granules) and localization (lipid droplets, vesicles, and SER) of organelles and inclusions. Moreover, embryos that have developed to excellent blastocysts presented further subtle deviations in ultrastructure affecting intercellular junctions and ribosome localization. Finally, we observed aberrant gene expression profile in SPOM blastocysts.

References

1. Pincus G, Enzmann EV. The comparative behavior of mammalian eggs in vivo and in vitro : I. the activation of ovarian eggs. J Exp Med. 1935;62:665–75.
2. Edwards RG. Maturation in vitro of mouse, sheep, cow, pig, rhesus monkey and human ovarian oocytes. Nature. 1965;208:349–51.
3. Fair T, Hyttel P, Greve T. Bovine oocyte diameter in relation to maturational competence and transcriptional activity. Mol Reprod Dev. 1995;42:437–42.
4. Hyttel P, Fair T, Callesen H, Greve T. Oocyte growth, capacitation and final maturation in cattle. Theriogenology. 1997;47:23–32.
5. Assey RJ, Hyttel P, Greve T, Purwantara B. Oocyte morphology in dominant and subordinate follicles. Mol Reprod Dev. 1994;37:335–44.
6. Holm P, Callesen H. In vivo versus in vitro produced bovine ova: similarities and differences relevant for practical application. Reprod Nutr Dev. 1998;38:579–94.
7. Zhang M, Su YQ, Sugiura K, Xia G, Eppig JJ. Granulosa cell ligand NPPC and its receptor NPR2 maintain meiotic arrest in mouse oocytes. Science. United States 2010. p. 366–9.
8. Vaccari S, Weeks JL, Hsieh M, Menniti FS, Conti M. Cyclic GMP signaling is involved in the luteinizing hormone-dependent meiotic maturation of mouse oocytes. Biol Reprod. 2009;81:595–604.
9. Norris RP, Ratzan WJ, Freudzon M, Mehlmann LM, Krall J, Movsesian MA, et al. Cyclic GMP from the surrounding somatic cells regulates cyclic AMP and meiosis in the mouse oocyte. Development. 2009;136:1869–78.
10. Richard FJ, Tsafriri A, Conti M. Role of phosphodiesterase type 3A in rat oocyte maturation. Biol Reprod. 2001;65:1444–51.

11. Dekel N, Beers WH. Rat oocyte maturation in vitro: relief of cyclic AMP inhibition by gonadotropins. Proc Natl Acad Sci U S A. 1978;75:4369–73.

12. Cho WK, Stern S, Biggers JD. Inhibitory effect of dibutyryl cAMP on mouse oocyte maturation in vitro. J Exp Zool. 1974;187:383–6.

13. Oliveira e Silva I, Vasconcelos RB, Caetano JV, Gulart LV, Camargo LS, Báo SN, et al. Induction of reversible meiosis arrest of bovine oocytes using a two-step procedure under defined and nondefined conditions. Theriogenology. 2011;75:1115–24.

14. Thomas RE, Thompson JG, Armstrong DT, Gilchrist RB. Effect of specific phosphodiesterase isoenzyme inhibitors during in vitro maturation of bovine oocytes on meiotic and developmental capacity. Biol Reprod. 2004;71:1142–9.

15. Ponderato N, Crotti G, Turini P, Duchi R, Galli C, Lazzari G. Embryonic and foetal development of bovine oocytes treated with a combination of butyrolactone I and roscovitine in an enriched medium prior to IVM and IVF. Mol Reprod Dev. 2002;62:513–8.

16. Luciano AM, Modina S, Vassena R, Milanesi E, Lauria A, Gandolfi F. Role of intracellular cyclic adenosine 3′,5′-monophosphate concentration and oocyte-cumulus cells communications on the acquisition of the developmental competence during in vitro maturation of bovine oocyte. Biol Reprod. 2004;70:465–72.

17. Franciosi F, Coticchio G, Lodde V, Tessaro I, Modina SC, Fadini R, et al. Natriuretic peptide precursor C delays meiotic resumption and sustains gap junction-mediated communication in bovine cumulus-enclosed oocytes. Biol Reprod. 2014;91:61.

18. Albuz FK, Sasseville M, Lane M, Armstrong DT, Thompson JG, Gilchrist RB. Simulated physiological oocyte maturation (SPOM): a novel in vitro maturation system that substantially improves embryo yield and pregnancy outcomes. Hum Reprod. 2010;25:2999–3011.

19. Gilchrist RB, Luciano AM, Richani D, Zeng HT, Wang X, Vos MD, et al. Oocyte maturation and quality: role of cyclic nucleotides. Reproduction. 2016;152:R143–57.

20. Hyttel P, Madsen I. Rapid method to prepare mammalian oocytes and embryos for transmission electron microscopy. Acta Anat (Basel). 1987;129:12–4.

21. Weibel ER, Kistler GS, Scherle WF. Practical stereological methods for morphometric cytology. J Cell Biol. 1966;30:23–38.

22. Dadarwal D, Adams GP, Hyttel P, Brogliatti GM, Caldwell S, Singh J. Organelle reorganization in bovine oocytes during dominant follicle growth and regression. Reprod Biol Endocrinol. 2015;13:124.

23. Zoller LC. A quantitative electron microscopic analysis of the membrana granulosa of rat preovulatory follicles. Acta Anat (Basel). 1984;118:218–23.

24. Baddeley AJ, Gundersen HJ, Cruz-Orive LM. Estimation of surface area from vertical sections. J Microsc. 1986;142:259–76.

25. Robertson I, Nelson R. Certification of the embryos. In: SM S, editor. Manual of the International Embryo Transfer Society. Savoy: Stringfellow DAS; 1998. p. 103–34.

26. Li HJ, Sutton-McDowall ML, Wang X, Sugimura S, Thompson JG, Gilchrist RB. Extending prematuration with cAMP modulators enhances the cumulus contribution to oocyte antioxidant defence and oocyte quality via gap junctions. Hum Reprod. 2016;31:810–21.

27. Shu YM, Zeng HT, Ren Z, Zhuang GL, Liang XY, Shen HW, et al. Effects of cilostamide and forskolin on the meiotic resumption and embryonic development of immature human oocytes. Hum Reprod. 2008;23:504–13.

28. Zeng HT, Ren Z, Guzman L, Wang X, Sutton-McDowall ML, Ritter LJ, et al. Heparin and cAMP modulators interact during pre-in vitro maturation to affect mouse and human oocyte meiosis and developmental competence. Hum Reprod. 2013;28:1536–45.

29. Zeng HT, Richani D, Sutton-McDowall ML, Ren Z, Smitz JE, Stokes Y, et al. Prematuration with cyclic adenosine monophosphate modulators alters cumulus cell and oocyte

30. metabolism and enhances developmental competence of in vitro-matured mouse oocytes. Biol Reprod. 2014;91:47.

30. Sutton-McDowall ML, Mottershead DG, Gardner DK, Gilchrist RB, Thompson JG. Metabolic differences in bovine cumulus-oocyte complexes matured in vitro in the presence or absence of follicle-stimulating hormone and bone morphogenetic protein 15. Biol Reprod. United States 2012. p. 87.

31. Kawashima I, Okazaki T, Noma N, Nishibori M, Yamashita Y, Shimada M. Sequential exposure of porcine cumulus cells to FSH and/or LH is critical for appropriate expression of steroidogenic and ovulation-related genes that impact oocyte maturation in vivo and in vitro. Reproduction. 2008;136:9–21.

32. Rose RD, Gilchrist RB, Kelly JM, Thompson JG, Sutton-McDowall ML. Regulation of sheep oocyte maturation using cAMP modulators. Theriogenology. 2013;79:142–8.

33. Guimarães AL, Pereira SA, Leme LO, Dode MA. Evaluation of the simulated physiological oocyte maturation system for improving bovine in vitro embryo production. Theriogenology. 2015;83:52–7.

34. Ulloa SM, Heinzmann J, Herrmann D, Timmermann B, Baulain U, Großfeld R, et al. Effects of different oocyte retrieval and in vitro maturation systems on bovine embryo development and quality. Zygote. 2015;23:367–77.

35. Bernal-Ulloa SM, Heinzmann J, Herrmann D, Hadeler KG, Aldag P, Winkler S, et al. Cyclic AMP affects oocyte maturation and embryo development in prepubertal and adult cattle. PLoS One. 2016;11:e0150264.

36. Hyttel P, Callesen H, Greve T. Ultrastructural features of preovulatory oocyte maturation in superovulated cattle. J Reprod Fertil. 1986;76:645–56.

37. Burkart A, Xiong B, Baibakov B, Jiménez-Movilla M, Dean J. Ovastacin, a cortical granule protease, cleaves ZP2 in the zona pellucida to prevent polyspermy. J Cell Biol. 2012;197:37–81.

38. Liu M. The biology and dynamics of mammalian cortical granules. Reprod Biol Endocrinol. 2011;9:149.

39. Reynier P, May-Panloup P, Chrétien MF, Morgan CJ, Jean M, Savagner F, et al. Mitochondrial DNA content affects the fertilizability of human oocytes. Mol Hum Reprod. 2001;7:425–9.

40. Yu Y, Dumollard R, Rossbach A, Lai FA, Swann K. Redistribution of mitochondria leads to bursts of ATP production during spontaneous mouse oocyte maturation. J Cell Physiol. 2010;224:672–80.

41. Stojkovic M, Machado SA, Stojkovic P, Zakhartchenko V, Hutzler P, Goncalves PB, et al. Mitochondrial distribution and adenosine triphosphate content of bovine oocytes before and after in vitro maturation: correlation with morphological criteria and developmental capacity after in vitro fertilization and culture. Biol Reprod. 2001;64:904–9.

42. Mohr LR, Trounson AO. Structural changes associated with freezing of bovine embryos. Biol Reprod. 1981;25:1009–25.

43. Mohr LR, Trounson AO. Comparative ultrastructure of hatched human, mouse and bovine blastocysts. J Reprod Fertil. 1982;66:499–504.

44. Vedeler A, Pryme IF, Hesketh JE. Insulin and step-up conditions cause a redistribution of polysomes among free, cytoskeletal-bound and membrane-bound fractions in Krebs II ascites cells. Cell Biol Int Rep. 1990;14:211–8.

45. Hesketh JE, Horne Z, Campbell GP. Immunohistochemical evidence for an association of ribosomes with microfilaments in 3T3 fibroblasts. Cell Biol Int Rep. 1991;15:141–50.

46. Larsen TH, Saetersdal T. Translocation of 60S ribosomal subunit in spreading cardiac myocytes. J Histochem Cytochem. 1998;46:963–70.

47. Tsai YJ, Lee HI, Lin A. Ribosome distribution in HeLa cells during the cell cycle. PLoS One. 2012;7:e32820.

48. Tiffin GJ, Rieger D, Betteridge KJ, Yadav BR, King WA. Glucose and glutamine metabolism in pre-attachment cattle embryos in

relation to sex and stage of development. J Reprod Fertil. 1991;93: 125–32.

49. Johnson MH, Nasr-Esfahani MH. Radical solutions and cultural problems: could free oxygen radicals be responsible for the impaired development of preimplantation mammalian embryos in vitro? BioEssays. 1994;16:31–8.

50. Dovolou E, Clemente M, Amiridis GS, Messinis IE, Kallitsaris A, Gutierrez-Adan A, et al. Effects of guaiazulene on in vitro bovine embryo production and on mRNA transcripts related to embryo quality. Reprod Domest Anim. 2011;46:862–9.

51. Ghanem N, Salilew-Wondim D, Gad A, Tesfaye D, Phatsara C, Tholen E, et al. Bovine blastocysts with developmental competence to term share similar expression of developmentally important genes although derived from different culture environments. Reproduction. England 2011. p. 551–64.

52. Zhang K, Haversat JM, Mager J. CTR9/PAF1c regulates molecular lineage identity, histone H3K36 trimethylation and genomic imprinting during preimplantation development. Dev Biol. 2013;383:15–27.

53. Smith C, Berg D, Beaumont S, Standley NT, Wells DN, Pfeffer PL. Simultaneous gene quantitation of multiple genes in individual bovine nuclear transfer blastocysts. Reproduction. England 2007. p. 231-42.

54. Harvey AJ, Navarrete Santos A, Kirstein M, Kind KL, Fischer B, Thompson JG. Differential expression of oxygen-regulated genes in bovine blastocysts. Mol Reprod Dev. 2007;74:290–9.

55. Dafni H, Larson PE, Hu S, Yoshihara HA, Ward CS, Venkatesh HS, et al. Hyperpolarized 13C spectroscopic imaging informs on hypoxia-inducible factor-1 and myc activity downstream of platelet-derived growth factor receptor. Cancer Res. 2010;70: 7400–10.

56. Cagnone GL, Dufort I, Vigneault C, Sirard MA. Differential gene expression profile in bovine blastocysts resulting from hyperglycemia exposure during early cleavage stages. Biol Reprod. 2012;86:50.

57. Semenza GL. Targeting HIF-1 for cancer therapy. Nat Rev Cancer. 2003;3:721–32.

58. Zhao YH, Zhou M, Liu H, Ding Y, Khong HT, Yu D, et al. Upregulation of lactate dehydrogenase a by ErbB2 through heat shock factor 1 promotes breast cancer cell glycolysis and growth. Oncogene. 2009;28:3689–701.

59. Hosseini SM, Dufort I, Caballero J, Moulavi F, Ghanaei HR, Sirard MA. Transcriptome profiling of bovine inner cell mass and trophectoderm derived from in vivo generated blastocysts. BMC Dev Biol. 2015;15:49.

60. Razza EM, Sudano MJ, Fontes PK, Franchi FF, Belaz KRA, Santos PH, et al. Treatment with cyclic adenosine monophosphate modulators prior to in vitro maturation alters the lipid composition and transcript profile of bovine cumulus? Oocyte complexes and blastocysts. Reprod Fertil Dev. 2018;30:1314.

61. Ferguson EM, Leese HJ. Triglyceride content of bovine oocytes and early embryos. J Reprod Fertil. 1999;116:373–8.

62. Sturmey RG, Reis A, Leese HJ, McEvoy TG. Role of fatty acids in energy provision during oocyte maturation and early embryo development. Reprod Domest Anim. 2009;44(Suppl 3):50–8.

63. Yao H, Ye J. Long chain acyl-CoA synthetase 3-mediated phosphatidylcholine synthesis is required for assembly of very low density lipoproteins in human hepatoma Huh7 cells. J Biol Chem. 2008;283:849–54.

64. Moon YA, Hammer RE, Horton JD. Deletion of ELOVL5 leads to fatty liver through activation of SREBP-1c in mice. J Lipid Res. 2009;50:412–23.

65. Miyazaki M, Dobrzyn A, Sampath H, Lee SH, Man WC, Chu K, et al. Reduced adiposity and liver steatosis by stearoyl-CoA desaturase deficiency are independent of peroxisome proliferator-activated receptor-alpha. J Biol Chem. 2004;279:35017–24.